Scaling laws for diamond chemical-vapor deposition. I. Diamond surface chemistry

D. G. Goodwin
Division of Engineering and Applied Science, California Institute of Technology, Pasadena, California 91125

(Received 14 June 1993; accepted for publication 21 August 1993)

A simplified model of the gas-surface chemistry occurring during chemical-vapor deposition of diamond thin films is presented. The model results in simple scaling relations, useful for process scale-up and optimization, for growth rate and defect density in terms of the local chemical environment at the substrate. A simple two-parameter expression for growth rate is obtained, which with suitable parameter choices reproduces the results of more detailed mechanisms and experiment over two orders of magnitude in growth rate. The defect formation model suggests that the achievable growth rate at specified defect density scales approximately quadratically with the atomic hydrogen concentration at the substrate.

I. INTRODUCTION

The chemical-vapor deposition (CVD) of polycrystalline diamond films has advanced to the point that thick, optically transparent films with thermal conductivity near that of natural type-IIa diamond may be synthesized. Due to its unique combination of hardness, optical transparency, high thermal conductivity, and high band gap, CVD diamond is uniquely suited to many challenging optical, electronic, and thermal management applications. Some examples currently being developed include heat spreaders for multichip modules,[1] cold cathodes,[2] infrared optical windows,[3] and coatings for cutting tools.[4] However, for CVD diamond to find widespread use in these applications, costs have to be significantly reduced.[5]

The contributions to the cost of CVD diamond include both fixed costs and the costs of process gases and energy. To minimize the fixed costs per carat of diamond produced, reactor throughput must be maximized, which requires achieving high film growth rates. To minimize the gas and energy costs, the process efficiency in converting raw feedstocks into diamond should be maximized. Which of these objectives is most important will depend on the growth process employed (for example, hot filament, microwave plasma, combustion flame, or arcjet).

In either case, if the growth conditions are altered to improve the growth rate or efficiency, it is necessary to know how this will affect film quality. Although current theoretical models can do a reasonable job of predicting growth rates for specified process conditions,[6,7] models to predict quality are rare[8–10] and are largely untested.

In this article a simplified model of the gas-surface chemistry occurring during diamond growth is developed. Although a detailed chemical mechanism of diamond growth would be complex, involving perhaps hundreds of reactions, the essence of diamond growth chemistry can be reduced to a few generic steps (essentially surface activation, adsorption on open sites, desorption, and incorporation into the lattice). By considering these steps alone, we arrive at a simple two-parameter rate law for diamond growth, which fits measured growth rates well with appropriate parameter choices. We also propose a simple defect formation model, which leads to a relation between growth rate, defect density, and atomic hydrogen concentration at the substrate. While no data currently exist against which to compare this relation, it agrees qualitatively with experience in film growth, and is simple enough that it is amenable to experimental test.

One conclusion of this analysis is that achieving high growth rates while maintaining film quality requires a high concentration of atomic hydrogen at the surface. This is made difficult by the rapid recombination of H on the diamond surface. In a companion article[11] the issue of atomic hydrogen transport to the substrate is considered in depth. Taken together, the simplified surface chemistry models presented here and the results for H transport in Ref. 11 result in scaling relations for growth rate and defect density in terms of controllable process parameters, and allow identification of the optimal conditions for high-rate growth of high-quality diamond.

Only "conventional" CVD diamond growth chemistry is considered here. The feedstock gas is assumed to be a dilute hydrocarbon in a carrier gas of H_2, and the substrate temperature is assumed to be near 1200 K. The effects of oxygen or halogens on diamond growth are not considered, largely because the chemistry occurring in these systems is not yet well understood. Also, the effect of substrate temperature, although large, is beyond the scope of this work. Finally, attention is confined primarily to the high-quality limit: It is assumed that the defect density is small enough that it is not necessary to account for large-scale nondiamond carbon formation.

In the sections below, we consider first the interactions of atomic hydrogen with the surface, resulting both in surface activation and catalytic recombination of H to H_2, followed by formulation of the reduced growth mechanism and defect formation model. Finally, these models are used to classify current growth processes.

 0021-8979/93/74(11)/6888/7/$6.00

II. SURFACE ACTIVATION

Diamond growth chemistry is initiated by abstraction of surface-terminating hydrogens by gas-phase atomic hydrogen:

$$C_dH + H \rightleftharpoons C_d^* + H_2. \quad (1)$$

Here C_dH represents a generic hydrogenated surface site and C_d^* the site with the hydrogen removed (a radical site). Radical sites may also be filled again with H via

$$C_d^* + H \rightarrow C_dH. \quad (2)$$

Due to the large negative change in free energy for reaction (2), the reverse process (thermal desorption of atomic hydrogen) is negligible. At steady state, the rate of creation of radical sites by reaction (1) just balances their rate of destruction by reactions (1) and (2). Solving for the steady-state radical fraction f^* yields

$$f^* = \frac{[C_d^*]}{[C_d^*]+[C_dH]} = \frac{k_1 X_H}{(k_1+k_2)X_H + k_{-1}}, \quad (3)$$

where k_i is the rate constant for reaction i, and X_H is the atomic hydrogen mole fraction at the surface. (It is assumed here that the background gas is primarily H_2, and thus $[H]/[H_2] = X_H$.) For X_H sufficiently large, Eq. (3) shows that f^* reaches a limiting value given by

$$f^* = \frac{k_1}{k_1+k_2}, \quad (4)$$

which is a function only of temperature. Since k_1/k_{-1} is equal to the equilibrium constant $K_{p,1}$ for reaction (1), Eq. (4) applies as long as

$$X_H \gg \left[\left(1+\frac{k_2}{k_1}\right)K_{p,1}\right]^{-1}. \quad (5)$$

To estimate k_1 and k_2, most studies have taken the approach introduced by Frenklach and Spear,[12] in which diamond surface chemistry is assumed to be similar to the chemistry of analogous gas-phase molecules (alkanes). A typical value for abstraction of a tertiary hydrogen from an alkane is[13]

$$k_1 \approx 1.3\times 10^{14} \exp(-7.3/RT) \ \text{cm}^3/\text{mol s}, \quad (6)$$

where $R = 1.99\times 10^{-3}$ kcal/mol/K.

The recombination rate constant k_2 may be estimated from the rate constants for H recombination with alkyl radicals. Since the diamond lattice provides a means to remove the enthalpy of recombination, the high-pressure limit of the gas-phase rate constants is most relevant. Data on H recombination with alkyl radicals are sparse. For the reaction $CH_3 + H \rightarrow CH_4$, Cobos and Troe[14] have recently concluded that the high-pressure recombination rate constant is 2×10^{14} cm^3/mol s, independent of temperature, with a factor of 2 uncertainty. (Although not an alkyl, the same value is reported by Ackermann *et al.*[15] for H recombination with the benzyl radical to form toluene.) However, for H recombination with the isopropyl radical i-C_3H_7, Warnatz[16] recommends a high-pressure rate constant of 2×10^{13} cm^3/mol s—an order of magnitude lower. Since in the gas phase the H atom may react with either side of the radical, while on a surface only one side is accessible, the gas-phase rate constant should be divided by 2 to estimate k_2. Therefore, the best estimates from gas-phase data are that k_2 is in the range 10^{13}–10^{14} cm^3/mol s.

It is often more convenient to work with gas-surface rate constants in units of reaction probability per site per collision, rather than the mass-action units of cm^3/mol s. (We will denote the rate constant in reaction probability units as γ_i.) Taking reaction (1) as an example, the conversion from k_i to γ_i may be done as follows. The probability per unit time that the hydrogen atom on a given C_dH site will be abstracted is simply $k_1[H]$. An alternate expression for the abstraction probability per unit time is $\gamma_1\Gamma_H/n_s$, where γ_1 is the abstraction probability per site per collision, Γ_H is the flux of atomic hydrogen striking the surface (mol/cm^2/s), and n_s is the total surface site density (mol/cm^2). Since $\Gamma_H = [H]\bar{c}_H/4$, where $\bar{c}_H$ is the mean thermal speed of a H atom, equating these two expressions for the abstraction probability leads to

$$\gamma_1 = \frac{4k_1 n_s}{\bar{c}_H}. \quad (7)$$

Using the value of n_s appropriate for the (111) surface (3×10^{-9} mol/cm^2), Eq. (6) is equivalent to

$$\gamma_1 \approx \frac{100}{\sqrt{T}} \exp(-7.3/RT). \quad (8)$$

At 1200 K, this expression yields $\gamma_1 \approx 0.14$.

From Eq. (7), at 1200 K a reaction probability per collision of 1.0 corresponds to a rate constant of 4×10^{13} cm^3/mol s. The gas-phase data for the recombination reaction would then suggest that γ_2 should be at least 0.25, and perhaps > 1.0. (Note that values greater than 1.0 are possible at low radical site coverage, since the domain of attraction for the reaction may exceed the distance to a neighboring hydrogenated site.) It is possible, however, that steric hindrances on the surface may impede recombination, resulting in a lower value for γ_2 than would be expected based on the gas-phase data.

An alternate approach to estimating γ_1 and γ_2 has been pursued by Brenner *et al.*, who have carried out molecular dynamics simulations of H interacting with the (111) surface,[17] using an empirical carbon-hydrogen potential.[18] This method has the advantage that realistic steric factors can be accounted for, as well as energy transfer to the lattice. The value for γ_1 they obtain (0.04 at 1200 K) is about a factor of 3 less than the value predicted by Eq. (8). For γ_2, they predict a value of 0.43 at 1200 K.

To estimate the value of X_H above which f^* reaches its limiting value, let us take $k_2/k_1 \approx 10$, based on the results of Brenner *et al.*[17] The best estimate to date of ΔG^0_{1200} for reaction (1) is -16 kcal/mol, calculated for the (100)(2 $\times$1):1H surface.[7] (For other surfaces, ΔG^0 should be within about 2 kcal/mol of this value.) Therefore, $K_{p,1} \approx 800$ at 1200 K. Using this value in Eq. (5), f^* should reach the saturation value for X_H above about 1×10^{-4}. Under filament-assisted growth conditions, the atomic hydrogen mole fraction has been measured to be

$\sim 1\times10^{-3}$ at the surface.[19–22] It is therefore likely that f^* is in the saturation regime under these conditions, and increasing the atomic hydrogen mole fraction at the surface will not result in greater surface activation. In the following sections, we assume that X_H is large enough at the surface that f^* is independent of gas composition.

III. HETEROGENEOUS RECOMBINATION OF ATOMIC HYDROGEN

In addition to activating the diamond surface, reactions (1) and (2) constitute a mechanism for surface-catalyzed recombination of H to H_2, since their sum is the reaction $2H\rightarrow H_2$. Because of surface recombination, H must be replenished by diffusion or convention to maintain a steady-state H concentration at the surface.

The surface recombination rate is specified by the recombination coefficient γ_H, which is defined as the probability that a H atom recombines when striking the surface. The H surface recombination rate is therefore

$$\dot{R}_H=\gamma_H\frac{[H]\bar{c}_H}{4}\ \text{mol/cm}^2\text{/s}. \tag{9}$$

We assume that recombination is first order,[23] and therefore γ_H is independent of [H]. Assuming the only two types of surface sites present are C_dH and C_d^*, then the recombination coefficient γ_H is simply

$$\gamma_H=(1-f^*)\gamma_1+f^*\gamma_2. \tag{10}$$

Substituting from Eq. (4) for f^*, this reduces to

$$\frac{1}{\gamma_H}=\frac{1}{2}\left(\frac{1}{\gamma_1}+\frac{1}{\gamma_2}\right), \tag{11}$$

which shows that the recombination coefficient is simply the harmonic mean of the abstraction and recombination probabilities. Note that if $\gamma_2\gg\gamma_1$, then $\gamma_H\approx2\gamma_1$, independent of γ_2.

Recently, direct measurements of γ_H on CVD diamond have been reported.[23–25] The reported values are shown in Fig. 1, along with theoretical estimates using Eq. (11). The measurements by Harris and Weiner at 1200 K and by Krasnoperov *et al.* at 1119 K are in reasonable agreement with the molecular dynamics results, and indicate that the value of γ_H at 1200 K is slightly greater than 0.1. The estimate of γ_H based on gas-phase rates appears to be somewhat too large; this may indicate that Eq. (8) overestimates the abstraction rate constant. In the high-temperature region, Krasnoperov *et al.* report a measured activation energy of 6.0 kcal/mol.[25] Near room temperature there is more scatter in the experimental data, which is apparently due to sample-to-sample variations.[26]

IV. A REDUCED MECHANISM FOR DIAMOND GROWTH

There is now considerable evidence that the dominant precursor to diamond is the methyl radical CH_3,[27–34] although diamond may grow from other species as well, notably acetylene,[32,33,35,36] with lower reaction rate. Several elementary mechanisms have been proposed for diamond growth both from methyl and acetylene[7,8,12,37–42] which consider in detail how the growth monomer (CH_3 or C_2H_2) may be added to a particular site type on a diamond surface through a series of elementary reactions.

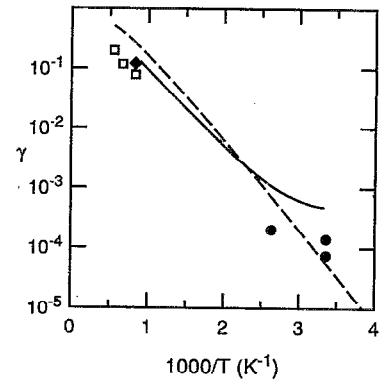

FIG. 1. Recombination coefficient of atomic hydrogen on the diamond surface. Measurements: Harris and Weiner (Ref. 23) (♦); Proudfit and Cappelli (Ref. 24) (●); Krasnoperov *et al.* (Ref. 25) (solid line). Theory: estimate for the (111) surface using Eq. (8) for γ_1 and assuming $\gamma_2=1.0$ (dashed line); estimate based on molecular dynamics simulation results for γ_1 and γ_2 for the (111) surface (Ref. 17) (□).

These studies have demonstrated that chemically reasonable means exist to add the growth species to the lattice, with growth rates similar to those measured;[7,39] however, they do not attempt to provide a complete description of diamond growth. For example, little work has been done on elementary mechanisms of defect formation, or on the development of the complex surface morphologies seen in scanning tunneling microscopy (STM) and atomic force microscopy (AFM) images.[43–48] Due to the complexity of these problems, progress in applying detailed kinetic mechanisms to issues such as defect formation is likely to be slow.

Alternatively, several groups[9,10,49] have begun formulating reduced mechanisms, which do not attempt to describe each step in detail, but seek to capture the correct qualitative behavior. In this way, entire classes of elementary reactions, occurring at multiple sites, are subsumed into a single, approximate overall reaction. By keeping the number of overall reactions to the minimum necessary, it is possible to derive simple analytical expressions for the growth rate and defect density, which may be compared to experiment. In this section, a simple reduced mechanism is developed which incorporates the most important features of more detailed mechanisms. In formulating this model, the simplest possible assumptions are made at each step, consistent with current knowledge of diamond growth chemistry.

The key processes that a reduced mechanism must account for are; (a) establishment of a steady-state surface radical site coverage via reactions (1) and (2); (b) attachment of reactive hydrocarbon species (unsaturated molecules or radicals) to the surface at these sites,

$$C_d^*+C_nH_m\xrightarrow{k_a}C_dA; \tag{12}$$

(c) removal back to the gas phase of the surface adsorbates, either by thermal desorption

$$C_dA \xrightarrow{k_d} C_d^* + C_nH_m, \tag{13}$$

or attack by atomic hydrogen (etching)

$$C_dA + qH \xrightarrow{k_e} C_d^* + \text{products}; \tag{14}$$

(d) incorporation of the adsorbate into the diamond lattice (with abstraction of adsorbate hydrogens by H),

$$C_dA + (m-1)H \xrightarrow{k_i} C_dH + (m-1)H_2. \tag{15}$$

While all proposed mechanisms contain steps similar to (a), (b), and (d), not all allow for removal of adsorbates [step (c)]; in fact, this step is critical for faceted film growth. For smooth crystal surfaces, incorporation must occur primarily at steps, which then move across the crystal face. This suggests that adsorbates which adsorb at terrace sites cannot incorporate at these sites—they must either migrate across the terrace to steps where they are incorporated, or must return to the gas phase. Since surface migration is expected to be negligible (due both to the large C—C bond strength and the termination of the surface with H),[50] the observation of faceted films indicates that return of adsorbates back to the gas phase, either through thermal desorption or etching, must occur during growth.

The above steps do not explicitly include mechanisms for nondiamond growth. It is assumed that conditions are such that high-quality diamond is being grown, and defect incorporation is a rare event. A simple model for defect formation is given in the following section.

It is clear that the incorporation reactions must involve atomic hydrogen, since the remaining hydrogens on the adsorbate must be removed by abstraction. In general, this will not occur in a single, elementary step, and thus the rate for this step may have a complicated dependence on [H]. However, for simplicity and in the absence of information to the contrary, the incorporation step is assumed to be first order in [H]. Similarly, it is assumed that the etching step is first order in [H].

Since incorporation occurs primarily at steps, k_i should be proportional to the step density f_s. It is assumed here, for simplicity, that the step density is constant.

With these assumptions, a simple kinetic expression may be written for the rate of change of the surface concentration of adsorbed hydrocarbons $[C_dA]$:

$$\frac{d[C_dA]}{dt} = k_a[C_nH_m][C_d^*] - k_d[C_dA] - (k_e + k_i)[C_dA][H]. \tag{16}$$

At steady state, $d[C_dA]/dt = 0$, and thus

$$[C_dA] = \frac{k_a[C_nH_m][C_d^*]}{k_d + (k_e + k_i)[H]}. \tag{17}$$

The incorporation rate $\dot{R}_C$ in mols/cm^2/s is simply

$$\dot{R}_C = k_i[C_dA][H]. \tag{18}$$

Dividing $\dot{R}_C$ by the molar density of diamond n_d (0.2939 mol/cm^3) gives the linear growth rate

$$G = \frac{k_i[C_dA][H]}{n_d}. \tag{19}$$

Substituting from Eq. (17) for $[C_dA]$ results in

$$G = \frac{g_1 f^*[C_nH_m][H]}{g_2 + [H]}, \tag{20}$$

where

$$g_1 = \frac{k_i k_a n_s}{(k_e + k_i) n_d} \tag{21}$$

and

$$g_2 = \frac{k_d}{k_e + k_i}. \tag{22}$$

Equation (20) shows that there exists a critical H concentration, equal to g_2, above which the growth rate is independent of [H] (assuming f^* is independent of X_H, as discussed above). The reasons for this behavior can be seen by examining the limiting cases $[H] \ll g_2$ and $[H] \gg g_2$. For $[H] \ll g_2$, the steady-state adsorbate concentration is determined by a balance between adsorption and thermal desorption, and therefore is independent of [H]. Since the incorporation rate is assumed first order in [H] [Eq. (18)], the growth rate is proportional to [H] in this limit. In the opposite limit ($[H] \gg g_2$), incorporation and etching are fast compared to thermal desorption, such that the steady-state adsorbate concentration is determined by the balance between adsorption and incorporation and/or etching. In this limit, $[C_dA]$ is inversely proportional to [H], and therefore the growth rate becomes independent of [H].

In previous numerical modeling work,[6,7] we have shown that a methyl growth mechanism proposed by Harris[39] leads to predicted growth rates within a factor of 2 both for low-rate methods (hot filament) and high-rate methods (oxyacetylene torch and dc arcjet). While the good absolute agreement with experiment is fortuitous, the reproduction of the correct scaling of the growth rate with gas composition is more significant. This mechanism considers reactions that convert the molecule bicyclononane to adamantane, and postulates that diamond growth on the (100) surface, where sites similar to the opposing hydrogen site on bicyclononane are present, proceeds in a similar manner. The original proposal considered the (100)(1 $\times$1):2H surface, but more recently Harris and Goodwin[7] have shown that this same mechanism is the rate-limiting portion of a more complex mechanism for growth on the (100)(2$\times$1):1H surface, which STM images[43] show is the predominant reconstruction present on the (100) face during CVD growth.

Although the Harris mechanism consists of 24 reactions (actually 12 reversible reactions), the growth rate predicted by this mechanism can be fit well by the functional form of Eq. (20), suggesting that the mechanism can be represented reasonably accurately by a smaller re-

TABLE I. A reduced methyl diamond growth mechanism. Units for k: cm^3, mol, s.

Reaction	k	γ	Notes
(s1) $C_dH+H\rightarrow C_d^*+H_2$	2.9×10^{12}	0.07	b,e
(s2) $C_d^*+H\rightarrow C_dH$	1.7×10^{13}	0.4	d,e
(s3) $C_d^*+CH_3\rightarrow C_dM$	3.3×10^{12}	0.31	c,e
(s4) $C_dM\rightarrow C_d^*+CH_3$	1.0×10^{4}	...	a,e
(s5) $C_dM+H\rightarrow C_dM^*+H_2$	2.0×10^{12}	0.05	c,e
(s6) $C_dM^*+H\rightarrow C_dH+C_d+H_2$	fast	fast	

[a]Arbitrarily set.
[b]Chosen to give $\gamma_H=0.12$.
[c]Chosen to reproduce Eq. (24).
[d]Chosen to match molecular-dynamics simulation results (Ref. 17).
[e]Substrate temperature is 1200 K.

duced mechanism. The growth rate in μm/h predicted by the Harris mechanism at 1200 K is well fit by the relation

$$G=9\times10^{11}f^*\frac{[CH_3][H]}{5\times10^{-9}+[H]}, \tag{23}$$

where the concentrations are in mol/cm^3. This simple expression reproduces the growth rate predicted by the Harris mechanism to within 10% over the range 3×10^{-10} mol/cm^3 $<[H]<10^{-5}$ mol/cm^3, 10^{-11} mol/cm^3 $<[CH_3]<10^{-6}$ mol/cm^3, over which range the growth rate varies from less than 0.1 μm/h to more than 7000 μm/h. Using the value of f^* predicted by this mechanism in the high-quality limit when the adsorbed methyl coverage is small ($f^*=0.2$) leads to

$$G=1.8\times10^{11}\frac{[CH_3][H]}{5\times10^{-9}+[H]}. \tag{24}$$

Whether or not the Harris mechanism provides a correct detailed description of diamond growth kinetics, Eq. (24) provides a simple relation which empirically predicts measured growth rates with reasonable accuracy.

For use with computational models, it is convenient to have a simple set of surface reactions which reproduces the growth rate of Eq. (24), and which also produces the correct recombination coefficient of H on diamond. Since the growth rate predicted by the reduced mechanism depends only on the parameters g_1f^* and g_2, many different sets of rate constants can reproduce Eq. (24); therefore, some rate constants can be set arbitrarily. Shown in Table I is one particular implementation of the general reduced mechanism [reactions (1), (2), (12)–(15)], designed to reproduce Eq. (24) and also give a H recombination coefficient $\gamma_H=0.12$. For reactions involving a gas-phase reactant, the rate constant is listed both in mass-action units and in units of reaction probability per collision per site.

In the mechanism shown in Table I, the etching rate constant k_e is arbitrarily set to zero, and k_d (reaction s4) is chosen to give an adsorbate lifetime on the surface of 100 μs.[7] Also, γ_2 is set to 0.4, to match molecular-dynamics simulation results,[17] and γ_1 is set to give the desired H recombination coefficient. The rate constants k_a and k_i (reactions s3 and s5, respectively) are then chosen to yield g_1f^* and g_2 values appropriate to Eq. (24). Note that C_dM represents an adsorbed methyl group, and C_d represents an atom of bulk diamond. The incorporation step is represented by the two elementary reactions (s5) and (s6). This is done to maintain the proper stoichiometry for the incorporation step ($C_dM+2H\rightarrow C_dH+C_d+2H_2$) while keeping it first order in [H]. The rate for (s6) is set to a large enough value that (s5) is always the rate-limiting step.

V. DEFECT GENERATION

The challenge in scaling CVD diamond processes to higher rates is to do so while maintaining high film quality (low defect density). To do this requires an understanding of how defect generation depends on the local chemical environment. There are many types of point and extended defects present in CVD diamond films (including sp^2 carbon, substitutional impurities, vacancies, interstitials, dislocations, twin planes, etc.[51]). At present there is little quantitative information relating defect densities to growth conditions.

Here a generic model of defect formation is developed which results in a simple scaling law for film quality. This model will clearly not apply to all types of defects. Nevertheless, its predictions are in qualitative accord with experience in film growth, and may be relevant in particular for hydrogen and sp^2 carbon incorporation.

The basic assumption of this model is that defects are generated when an adsorbate reacts with a nearby adsorbate before it is fully incorporated into the lattice. For example, two neighboring adsorbed methyl groups could react to form an sp^2 ethylenelike group, which then could be overgrown to lock in an sp^2 defect.

The rate of defect generation $\dot{R}_{def}$ (mol/cm^2/s) is assumed to be proportional to the number of adsorbate pairs on the surface. Assuming randomly distributed adsorbates,

$$\dot{R}_{def}=k_{def}[C_dA]^2, \tag{25}$$

where k_{def} is the (temperature-dependent) rate constant for defect formation. The defect fraction in the film X_{def} is given by the defect formation rate divided by the rate of sp^3 carbon incorporation,

$$X_{def}=\frac{\dot{R}_{def}}{\dot{R}_C}. \tag{26}$$

Substituting for $[C_dA]$ from Eq. (19) and using $\dot{R}_C=n_dG$, results in

$$X_{def}=\left(\frac{n_dk_{def}}{k_i^2}\right)\frac{G}{[H]^2}. \tag{27}$$

At constant substrate temperature, then,

$$X_{def}\propto\frac{G}{[H]^2}. \tag{28}$$

Equation (28) provides a very simple expression relating film quality, growth rate, and the atomic hydrogen concentration at the substrate. The qualitative predictions of Eq. (28)—that film quality and growth rate are inversely related, and that increasing atomic hydrogen at the surface improves film quality—are in accord with experi-

ence in a wide variety of growth environments. However, it must be emphasized that the quantitative validity of this expression is unclear, and at present there exist no known experimental data available to directly test Eq. (28). In particular, the exponent in the denominator depends on two assumptions—that defect formation is zeroth order in [H] [Eq. (25)] and that incorporation into the lattice is first order in [H] [Eq. (18)]. A less specific generalization of this relation would be

$$X_{\text{def}} \propto \frac{G}{[\text{H}]^n}, \tag{29}$$

where n must be determined experimentally.

Some insight into the appropriate value for n can be gained by examining the predictions of Eq. (29) for conventional filament-assisted diamond growth. In this environment at 20 Torr, the H concentration at the surface is approximately 5×10^{-10} mol/cm^3,[19,20] and therefore from Eq. (23) the growth rate is proportional to $[CH_3][H]$. Equation (29) then becomes

$$X_{\text{def}} \propto \frac{[\text{CH}_3]}{[\text{H}]^{n-1}}. \tag{30}$$

Under these conditions, the gas-phase reaction

$$\text{CH}_4+\text{H}\rightleftharpoons\text{CH}_3+\text{H}_2 \tag{31}$$

is rapid and near partial equilibrium.[20,52] As a consequence, $[CH_3]$ is approximately proportional to $[CH_4][H]/[H_2]$, which implies that

$$X_{\text{def}} \propto \frac{[\text{CH}_4]}{[\text{H}_2][\text{H}]^{n-2}} \tag{32}$$

for typical hot-filament conditions. Taking the value $n=2$ leads to the prediction that the defect density at a given substrate temperature is determined primarily by the input methane fraction—a result in accord with much experience with filament-assisted reactors. Therefore, while the theoretical justification for Eq. (28) is tenuous, it at least leads to reasonable predictions for filament-assisted conditions.

VI. PROCESS MAP

The simplified models discussed above indicate that the growth rate and defect density, for a given temperature, are functions only of the H and CH_3 concentrations at the substrate. In Fig. 2, contours of constant growth rate, calculated from Eq. (24), are shown, along with contours of constant $G/[H]^2$ (normalized to hot-filament conditions), which provides a measure of relative defect density. Typical concentration regimes of most common diamond CVD methods are also shown. For the hot-filament and microwave plasma cases, the concentrations are taken from the measurements of Hsu.[19–21] For the other processes shown, the H and CH_3 concentrations are estimates based on numerical simulations.[6,53]

Several points are apparent from Fig. 2. First of all, it is seen that standard low-pressure (20 Torr) hot-filament and low power (800 W) microwave plasma systems operate in a regime in which the growth rate is dependent on

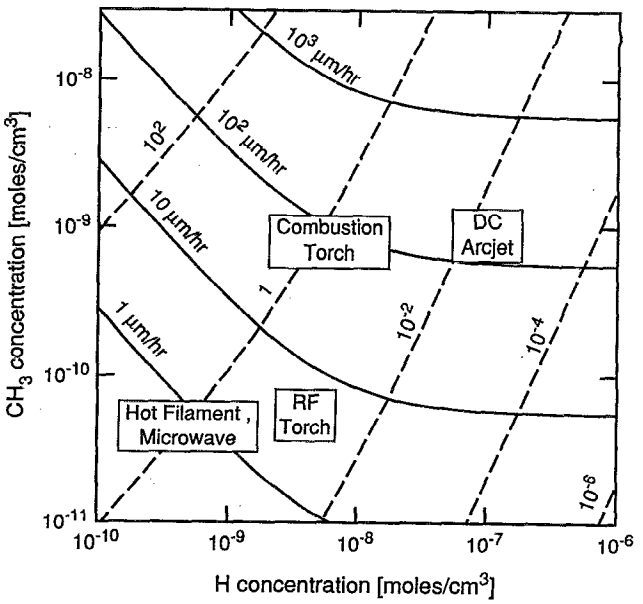

FIG. 2. Contours of constant growth rate from Eq. (24) (solid lines) and of constant relative defect density from Eq. (28) (dashed lines) vs the methyl and H concentrations at the surface. Typical operating regimes for some common diamond CVD processes are also shown (Refs. 6, 19–21, 53). The hot-filament and microwave values are for typical low power diffusion-dominated reactors at 20 Torr. The combustion torch values are for an acetylene-oxygen flame at 1 atm with $C_2H_2/O_2=1.1$. The pressures for the rf torch and dc arcjet are 1 atm and 220 Torr, respectively.

[H], as discussed above. On the other hand, arcjet reactors may operate well into the saturated regime. Here the growth rate is independent of [H], but film quality still improves with increasing [H]. Atmospheric pressure combustion torches and rf plasma torches operate in a transitional regime between these two limits.

The results of Fig. 2 also suggest that the film quality is similar for hot-filament, microwave, and combustion torch films grown at an acetylene to oxygen ratio $R=1.1$ (although the effect of oxygen on quality is not considered here). In general, as the CH_3 concentration is increased at constant [H], both growth rate and defect density increase. These results indicate that, in the absence of oxygen or halogen addition, the highest-quality diamond should be grown in high-speed plasma jet reactors, due to the high H concentrations at the surface achievable in these systems. They also suggest that it should be possible in such plasma systems to use gas compositions significantly richer in hydrocarbons than is possible in most other methods, again due to the large [H] at the surface.

These results show that achieving high growth rates while maintaining film quality requires delivering a large amount of atomic hydrogen to the substrate. In fact, the H concentration at the surface is the primary factor limiting the achievable growth rate for a specified film quality. Once [H] is fixed, the methyl concentration may be easily set by adjusting the methane fraction in the feed gas to give the desired growth rate and/or defect density.

ACKNOWLEDGMENTS

The author would like to thank Dr. Steve Harris, Dr. Lev Krasnoperov, and Dr. Mark Cappelli for providing copies of their work prior to publication. This work is supported, in part, by the National Science Foundation, the Office of Naval Research, and the Naval Research Laboratory.

[1] R. C. Eden, in *Applications of Diamond Films and Related Materials*, edited by Y. Tzeng, M. Yoshikawa, M. Murakawa, and A. Feldman (Elsevier, Amsterdam, 1991), pp. 259–266.
[2] M. W. Geis and J. C. Angus, Sci. Am. **267**, 84 (1992).
[3] C. Willingham, T. Hartnett, C. Robinson, and C. Klein, in *Applications of Diamond Films and Related Materials*, edited by Y. Tzeng, M. Yoshikawa, M. Murakawa, and A. Feldman (Elsevier, Amsterdam, 1991), pp. 157–162.
[4] S. Yazu and T. Nakai, in *Applications of Diamond Films and Related Materials*, edited by Y. Tzeng, M. Yoshikawa, M. Murakawa, and A. Feldman (Elsevier, Amsterdam, 1991), pp. 37–42.
[5] J. P. Dismukes, J. V. Busch, N. V. Nallicheri, and K. R. Walton, in *Applications of Diamond Films and Related Materials*, edited by Y. Tzeng, M. Yoshikawa, M. Murakawa, and A. Feldman (Elsevier, Amsterdam, 1991), pp. 635–644.
[6] D. G. Goodwin, Appl. Phys. Lett. **59**, 277 (1991).
[7] S. J. Harris and D. G. Goodwin, J. Phys. Chem. **97**, 23 (1993).
[8] M. Frenklach and H. Wang, Phys. Rev. B **43**, 1520 (1991).
[9] J. E. Butler and R. L. Woodin, Philos. Trans. R. Soc. London **342**, 209 (1993).
[10] M. H. Loh and M. A. Cappelli, Diamond Related Mater. **2**, 454 (1993).
[11] D. G. Goodwin, J. Appl. Phys. **74**, 6895 (1993).
[12] M. Frenklach and K. E. Spear, J. Mater. Res. **3**, 133 (1991).
[13] C. K. Westbrook, J. Warnatz, and W. J. Pitz, in *Twenty-second Symposium (International) on Combustion* (The Combustion Institute, Pittsburgh, 1988), p. 893.
[14] C. J. Cobos and J. Troe, Z. Phys. Chem. Neue Folge **167**, 129 (1990).
[15] L. Ackermann, H. Hippler, P. Pagsberg, Ch. Reihs, and J. Troe, J. Phys. Chem. **94**, 5247 (1990).
[16] J. Warnatz, in *Combustion Chemistry*, edited by W. C. Gardiner, Jr. (Springer, New York, 1984), p. 197.
[17] D. W. Brenner, D. H. Robertson, R. J. Carty, D. Srivastava, and B. J. Garrison, in *Computational Methods in Materials Science*, edited by J. E. Mark, M. E. Glicksman, and S. P. Marsh (Materials Research Society, Pittsburgh, PA, 1992), pp. 255–260.
[18] D. W. Brenner, Phys. Rev. B **42**, 9458 (1990).
[19] W. L. Hsu, in *Proceedings of the 2nd International Symposium on Diamond and Related Materials*, edited by A. J. Purdes, K. E. Spear, B. S. Meyerson, M. Yoder, R. Davis, and J. C. Angus (The Electrochemical Society, Pennington, NJ, 1991), pp. 217–223.
[20] W. L. Hsu, Appl. Phys. Lett. **59**, 1427 (1991).
[21] W. L. Hsu, J. Appl. Phys. **72**, 3102 (1992).
[22] W. L. Hsu and D. M. Tung, Rev. Sci. Instrum. **63**, 4138 (1992).
[23] S. J. Harris and A. M. Weiner, J. Appl. Phys. **74**, 1022 (1993).
[24] J. A. Proudfit and M. A. Cappelli, in *Proceedings of the 3rd International Symposium on Diamond Materials*, edited by A. J. Purdes, K. E. Spear, B. S. Meyerson, M. Yoder, R. Davis, and J. C. Angus (The Electrochemical Society, Pennington, NJ, in press).
[25] L. N. Krasnoperov, I. J. Kalinovski, D. Gutman, and H. N. Chu (unpublished).
[26] L. N. Krasnoperov (personal communication).
[27] C. J. Chu, M. P. D'Evelyn, R. H. Hauge, and J. L. Margrave, J. Mater. Res. **5**, 2405 (1990).
[28] C. J. Chu, M. P. D'Evelyn, R. H. Hauge, and J. L. Margrave, J. Appl. Phys. **70**, 1695 (1991).
[29] M. P. D'Evelyn, C. J. Chu, R. H. Hauge, and J. L. Margrave, J. Appl. Phys. **71**, 1528 (1992).
[30] S. J. Harris and A. M. Weiner, Thin Solid Films **212**, 201 (1992).
[31] S. J. Harris and A. M. Weiner, J. Appl. Phys. **70**, 1385 (1991).
[32] L. R. Martin and M. W. Hill, J. Mater. Sci. Lett. **9**, 621 (1990).
[33] S. J. Harris and L. R. Martin, J. Mater. Res. **5**, 2313 (1990).
[34] C. E. Johnson, W. A. Weimer, and F. M. Cerio, J. Mater. Res. **7**, 1427 (1992).
[35] L. R. Martin, J. Mater. Sci. Lett. **12**, 246 (1993).
[36] M. H. Loh and M. A. Cappelli, in *Proceedings of the 3rd International Symposium on Diamond Materials*, edited by A. J. Purdes, K. E. Spear, B. S. Meyerson, M. Yoder, R. Davis, and J. C. Angus (The Electrochemical Society, Pennington, NJ, in press).
[37] D. Huang and M. Frenklach, J. Phys. Chem. **96**, 1868 (1992).
[38] D. Huang, M. Frenklach, and M. Maroncelli, J. Phys. Chem. **92**, 6379 (1988).
[39] S. J. Harris, Appl. Phys. Lett. **56**, 2298 (1990).
[40] D. N. Belton and S. J. Harris, J. Chem. Phys. **96**, 2371 (1992).
[41] S. J. Harris and D. N. Belton, Thin Solid Films **212**, 193 (1992).
[42] B. J. Garrison, E. J. Dawnkaski, D. Srivastava, and D. W. Brenner, Science **255**, 835 (1992).
[43] T. Tsuno, T. Imai, Y. Nishibayashi, K. Hamada, and N. Fujimori, Jpn. J. Appl. Phys. **30**, 1063 (1991).
[44] H. G. Busmann, H. Sprang, I. V. Hertel, W. Zimmermann-Edling, and H. J. Güntherodt, Appl. Phys. Lett. **59**, 295 (1991).
[45] V. Baranauskas, M. Fukui, C. R. Rodrigues, N. Parizotto, and V. J. Trava-Airoldi, Appl. Phys. Lett. **60**, 1567 (1992).
[46] H. G. Maguire, M. Kamo, H. P. Lang, and H. J. Güntherodt, Appl. Surf. Sci. **60**, 301 (1992).
[47] L. F. Sutcu, M. S. Thomson, C. J. Chu, R. H. Hauge, J. L. Margrave, and M. P. D'Evelyn, Appl. Phys. Lett. **60**, 1685 (1992).
[48] L. F. Sutcu, C. J. Chu, M. S. Thompson, R. H. Hauge, J. L. Margrave, and M. P. D'Evelyn, J. Appl. Phys. **71**, 5930 (1992).
[49] J. C. Angus (personal communication).
[50] S. P. Mehandru and A. B. Anderson, Surf. Sci. **248**, 369 (1991).
[51] G. H. Ma, B. E. Williams, J. T. Glass, and J. T. Prater, Diamond Related Mater. **1**, 25 (1991).
[52] D. G. Goodwin and G. G. Gavillet, J. Appl. Phys. **68**, 6393 (1990).
[53] T. G. Owano, C. H. Kruger, and D. G. Goodwin (unpublished).